ANL-6403

Argonne National Laboratory

FAST REACTOR SHAPE FACTORS AND SHAPE-DEPENDENT VARIABLES

by

W. B. Loewenstein
and G. W. Main

ANL-6403
Reactor Technology
(TID-4500, 16th Ed.,
Amended)
AEC Research and
Development Report

ARGONNE NATIONAL LABORATORY
9700 South Cass Avenue
Argonne, Illinois

FAST REACTOR SHAPE FACTORS AND SHAPE-DEPENDENT VARIABLES

by

W. B. Loewenstein and G. W. Main

Reactor Engineering Division

November 1961

Operated by The University of Chicago
under
Contract W-31-109-eng-38

TABLE OF CONTENTS

LIST OF FIGURES

LIST OF TABLES

FAST REACTOR SHAPE FACTORS AND SHAPE-DEPENDENT VARIABLES

by

W. B. Loewenstein and G. W. Main

ABSTRACT

Existing experimental data on the variation of reactivity with core geometry are reviewed. Four typical fast neutron systems are analyzed to predict:

1. the variation of critical mass with cylindrical core geometry (core and reflector composition are held fixed);
2. the reactivity worth of fuel at the radial core boundary as a function of cylindrical core geometry;
3. the geometric variation of heat removal parameters; these include the ratio of:
   a. Maximum power density to average power density in the core.
   b. Maximum power density to average radial power density in the core.
   c. Total reflector power to total core power.

The absolute values of all of these parameters are determined by the core and reflector compositions of the four systems. These were chosen to simulate typical constituents of interest to reactor analysis.

Two systems represent a typical fast reactor and a typical fast critical experiment. The other two systems represent compositional combinations of the two basic systems.

The results of the analyses show that the significant geometric variation is in items 2 and 3b. Item 1 is almost constant for small variations near the optimum geometric configuration. Outside of this range, the variation of critical mass with core geometry is pronounced.

A most significant result shows that the ratio of the spherical critical mass to the minimum cylindrical critical mass, for fixed core and reflector composition, depends primarily on core composition. The composition of the thick reflector has a lesser effect on this ratio which was found to increase with core density.

The two-dimensional calculations are interpreted and analyzed on the basis of one-dimensional concepts. Reflector savings are calculated for spherical and cylindrical systems. The more exact reflector savings determinations are compared with more approximate calculations. It is found that the approximate determinations are qualitatively correct and show correct trends. However, the more detailed and accurate analytical techniques are required for precision comparison between theory and experiment.

An interesting correlation between critical mass and core surface area is demonstrated. It was found that, in the range of interest, the critical mass depends almost linearly upon the surface area. The same linear dependence approximates all the systems studied.

I. INTRODUCTION

A large fraction of the reported fast neutron critical experiments were investigated in cylindrical geometry.[1,2] Analytical efforts to interpret the experimental data and test microscopic multigroup constants utilize reflected spherical geometry.[3,4,5] It has been demonstrated[1-7] that spherical calculations do give the spectral properties of the cylindrical critical assemblies. However, there must be a basis for converting the predicted spherical critical mass to cylindrical geometry for comparison with the experimental data. This is generally accomplished by the use of a suitable Shape Factor.

The Shape Factor (S.F.)* is defined as the ratio of the spherical critical mass of a system to the critical mass of a given assembly.** Both systems have identical core compositions and similar reflector parameters.

Survey analyses of a series of critical experiments often resort to the reported experimental Shape Factors (see Fig. 6-2 of Ref. 8). These limited data suggest that for the fairly well reflected and moderately sized systems, the optimum geometry† Shape Factor is relatively independent of core size or composition.

The analysis of fast neutron critical experiments performed at ZPR-III has shown that fair predictions may be made for systems having high-density uranium cores.[4] Good predictions are not made for those systems with low-density cores (due to the presence of coolant and structural materials).[4,5] Predictions for the low-density system can be improved by more sophisticated averaging of cross sections over scattering resonances.[9] However, such averaging does not bring agreement between theory and experiment with the precision found for the high-density system.[5]

The apparent lack of agreement between theory and experiment for the low-density systems suggests that the shape conversion, from spherical to cylindrical geometry, may be dependent on the core and reflector densities as well as the core size and configuration. The question is: How significant is the variation of the optimum geometry Shape Factor? A reliable analytical technique must be used to unambiguously answer this question.

---

* The Shape Factor is sometimes specified to be the inverse of this definition.

** The assembly core usually has simple cylindrical or rectangular geometry but may conceivably have very irregular geometry.

† Minimum Cylindrical Critical Mass.

Initial efforts were devoted to predicting the existing experimental data on 50-liter optimum geometry cores.(1) These showed that both one- and two-dimensional diffusion theory could, to a fairly high degree of precision, predict the criticality of the known systems (see Tables 18 and 22 of Ref. 1). The two-dimensional calculations were straightforward. The one-dimensional analyses assumed that the neutron flux ϕ is approximately separable:

$$\phi(r,z) \approx R(r)Z(z) \quad .$$

With this assumption, one-dimensional calculations (axially bare, radially reflected cylinders and radially bare, axially reflected slabs) were performed to yield the following relationships:

$$b_r^2 = \alpha_r C + \beta_r \quad , \tag{1}$$

$$b_z^2 = \alpha_z C + \beta_z \quad , \tag{2}$$

where b_r^2 is the radial buckling, b_z^2 is the axial buckling and C is the enrichment (U^{235} in U) of the fuel. The quantities α_r, β_r, α_z, and β_z are constants. Fundamental mode calculations with various core enrichments yield the material buckling κ^2 of the core:

$$\kappa^2 = \alpha C + \beta \quad . \tag{3}$$

Equations (1), (2), and (3) along with the constraint

$$b_r^2 + b_z^2 - \kappa^2 = 0 \tag{4}$$

allow for the solution of the critical enrichment which satisfies the self-consistent set of calculations. Then b_r^2 and b_z^2 for the critical enrichment specify the appropriate axial and radial reflector saving.

The one-dimensional method of solution showed that both axial and radial reflector saving are a function of the ratio of core height to diameter (see Table 6-14 of Ref. 8).

A series of detailed calculations were performed to compare the approximate one-dimensional method with the more accurate two-dimensional method. The results showed (see Table 18 of Ref. 3) that

$$-0.01 < \frac{k_{1D} - k_{2D}}{k_{2D}} < +0.03$$

for uniformly reflected systems. Here k_{1D} and k_{2D} are the calculated multiplication constants for one- and two-dimensional analyses, respectively.

The expected variation in the shape conversion factors is expected to represent about 1% $\Delta k/k$. Therefore, a precise analysis to resolve this question requires two-dimensional methods.

The Shape Factor is useful for fast reactor design. Conceptual studies, usually performed in idealized spherical geometry, tend to minimize the required fuel inventory.

The fuel inventory doubling time in a fast power breeder reactor is directly proportional to the critical mass and inversely proportional to the total power. The critical mass is a function of the Shape Factor. The total power may be a function of the Shape Factor. For instance, the maximum power density may be increased as the core dimensions parallel to coolant channels are reduced. The Shape Factor may be used to determine fuel doubling time for an actual reactor from that predicted by the general conceptual studies.

II. EXPERIMENTAL DATA

A variety of Shape Factor investigations have been reported, most for cylindrical geometry. They may be of limited use for general fast reactor design. It is not obvious that they are always applicable.

The experimental data include those for:

1. High-density, δ-phase plutonium cores[10] reflected by either natural uranium or beryllium. Reflector thicknesses were 2.0 and 5.0 cm. The data are shown in Fig. 1.

2. High-density, highly enriched (~93%) uranium cores reflected by natural uranium,[11] water,[12] and graphite.[12] Natural uranium thicknesses were 2.84, 5.08 and 20.3 cm. The graphite thickness was $>$ 40 cm. The water reflector was essentially infinite. Unreflected systems were also included. These data are shown in Fig. 2.

3. EBR-II[13,14] size and composition cores reflected by high-density depleted uranium. The reflector thickness was ~30 cm. The core contained about 30 v/o uranium (~46% enriched), 31 v/o aluminum, and 12 v/o stainless steel.[1] Figure 3 includes these data.

4. Several cores containing 49 v/o uranium (~23% enriched), 21 v/o aluminum and 15 v/o stainless steel. The reflector is ~30 cm of the high density depleted uranium.[1] These data are also shown on Fig. 3.

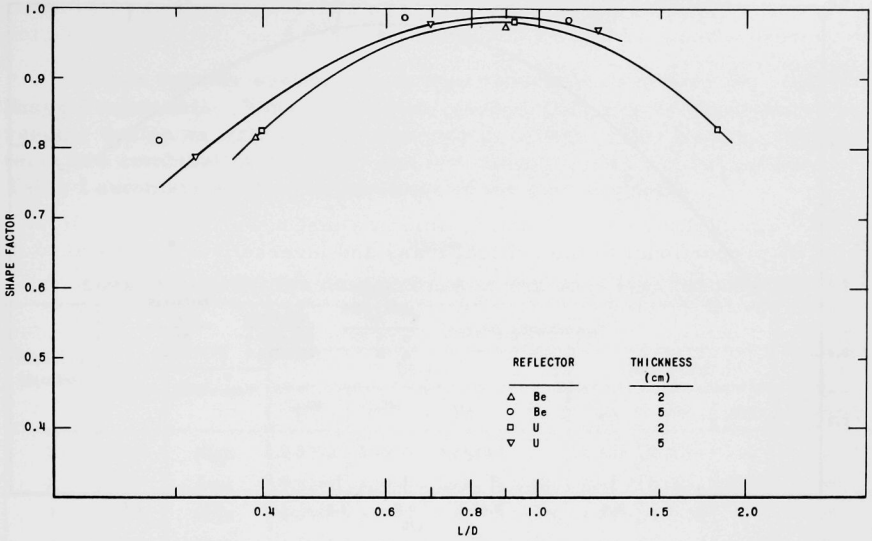

FIG. 1
SHAPE FACTORS FOR HIGH DENSITY PLUTONIUM CORES
(MEASURED AT UCRL)

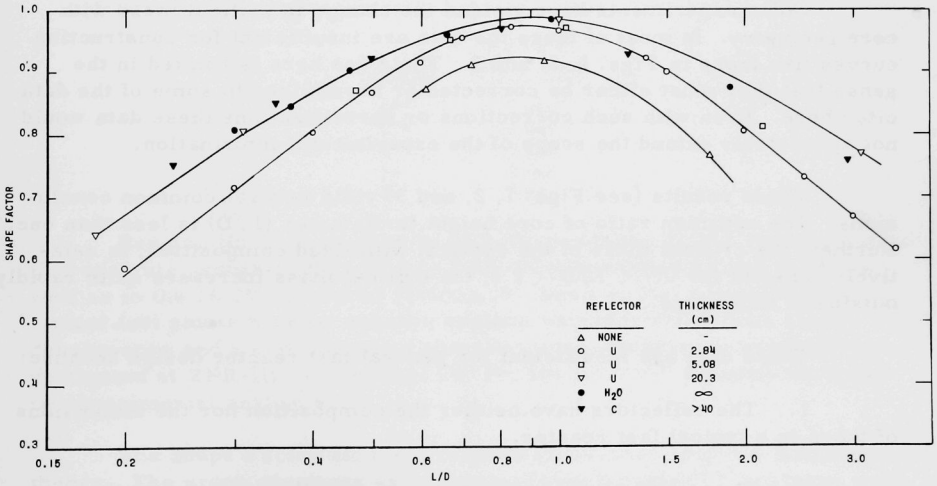

FIG. 2
SHAPE FACTORS FOR
HIGH DENSITY, HIGHLY ENRICHED URANIUM CORES
(MEASURED AT LASL)

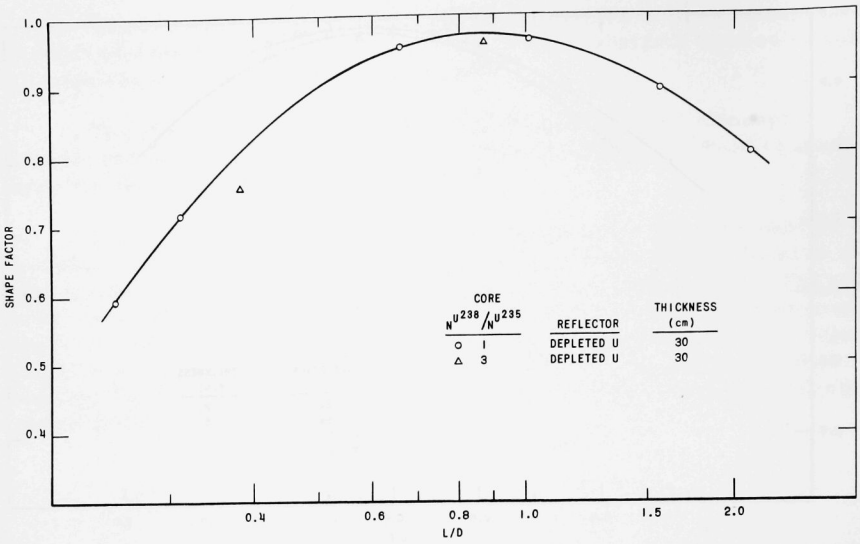

FIG. 3
SHAPE FACTORS FOR SMALL DILUTE CORES
(MEASURED AT ZPR-III)

Other experiments have yielded the change in critical mass with core geometry. In most of these the data are insufficient for constructing curves like those in Figs. 1, 2, and 3. Their use here is limited in the sense that they must either be corrected or normalized to some of the data cited here. Even with such corrections or normalizations these data would not appreciably extend the scope of the experimental information.

These results (see Figs. 1, 2, and 3) yield several common conclusions. The optimum ratio of core height to diameter (L/D) is less than one. Further, the critical mass of the system, with fixed composition, is relatively constant for $0.7 < L/D < 1.1$; the critical mass increases quite rapidly outside of this range.

These data are insufficient for general fast reactor design because:

1. The reflectors have neither the composition nor the dimensions of those in a typical fast reactor.

2. The experimental cores are quite small in relation to the currently conceived fast power reactors.[15] The experimental data for the EBR-II size represent the largest cores (~50 liters in optimum geometry) reported to date. Current conceptual studies deal primarily with core volumes greater than 400 liters.

III. PREDICTED SHAPE FACTORS FOR FOUR FAST NEUTRON SYSTEMS

Four reactor systems have been extensively analyzed for typical Shape Factor data. These represent systems that may be encountered in reactor design as well as in an analysis of critical experiments. The systems are combinations of high- and low-density cores and reflectors. Table I summarizes the compositions of the four systems.

Table I

CORE AND REFLECTOR COMPOSITIONS OF THE FOUR REACTOR SYSTEMS

Reactor Number	Density		Volume Fractions*							Approx. Spherical Core Volume (liters)
			Core				Reflector			
	Core	Reflector	U^{235}	U^{238}	Fe	Na	U	Fe	Na	
1	High	High	0.0712	0.7405	0.0928	0	0.835	0.0731	0	560
2	Low	Low	0.0447	0.2553	0.20	0.50	0.60	0.20	0.20	850
3	Low	High	0.0581	0.0914	0.245	0.376	0.835	0.0731	0	380
4	High	Low	0.0712	0.7405	0.0928	0	0.60	0.20	0.20	550

* Volume Fraction x 100 = Volume %; the total volume fraction is not unity because voids exist.

Reference atomic densities (N) are:

Material	N x 10^{-24} (atoms/cm^3)
U^{235}	0.048
U^{238}	0.048
U	0.048
Fe	0.085
Na	0.022

Reactor No. 1 is similar to ZPR-III Assembly 25.[2] Results from this analysis probably will apply to ZPR-III Assemblies 22 and 24,[2] as well as to the 16.25% enriched Jemima.[6] Reactor No. 2 represents a typical fast power breeder reactor system. Reactor No. 3, with a low-density core and a high-density reflector, is typical of many systems investigated at ZPR-III (Assemblies 15, 29, 30, 31).[1,2] Reactor No. 4 has no experimental analogue.

The Shape Factor analyses utilized three-energy-group diffusion theory. The group constants are given in Table II. PDQ[16] analyses were used to obtain results in cylindrical geometry; calculations for spherical geometry were performed with RE-122.[17]

Table II

THREE-GROUP FAST CROSS SECTIONS

	j*	ν	$\nu\sigma_f$	σ_{tr}	σ_a	$\sigma_{j \rightarrow j+1}$
U^{235}	1	2.65	3.44	4.93	1.4	1.4
	2	2.5	3.50	6.0	1.7	-
	3	2.5	15.00	19.0	9.0	-
U^{238}	1	2.8	1.48	4.93	0.57	2.1
	2	-	-	7.0	0.18	-
	3	-	-	20.0	0.80	-
Fe	1	-	-	2.2	0.0025	0.74
	2	-	-	2.9	0.0057	0.0025
	3	-	-	7.5	0.015	-
Na	1	-	-	2.0	0.0002	0.4
	2	-	-	3.5	0.0010	0.1
	3	-	-	10.0	0.0015	-

*j = 1: 1.35 Mev $\leq E < \infty$

j = 2: 9.1 kev $\leq E \leq$ 1.35 Mev

j = 3: 1 kev $\leq E \leq$ 9.1 kev

The analytical procedure was the following:

1. With fixed composition core and reflector, the spherical core radius was varied until criticality was attained.

2. The experimental Shape Factor curves (see Fig. 3) were then used to specify the core dimension for the initial calculations in cylindrical geometry.

3. The results from step 2 were then used to specify a critical core configuration.

4. If the result of step 3 was not critical, the final results were interpolated to give a critical value for L/D.

5. In two cases (Reactors 1 and 2), the predicted curve was used to specify the height and diameter of a critical core. The resulting reactors were analyzed with PDQ and found to be critical within 0.1% $\Delta k/k$.

Table III is a summary of the individual calculations. Table IV and Figs. 4 and 5 show the final results of these analyses. It may be seen that the optimum geometry Shape Factor is a function of the reactor system used. It is clearly not an invariant quantity. Furthermore, the variation of critical mass with core geometry also is a function of the specific reactor system.

Table III

SUMMARY OF SPECIFIC REACTOR CALCULATIONS

Reactor No.	Extrapolated Critical Value of L/D	First Calculation					Second Calculation				Perturbation of Core Boundary	
		Core Volume (liters)	Core Height* (cm)	Core Diameter (cm)	L/D**	Calculated k_{eff}	Core Volume (liters)	Core Diameter (cm)	L/D**	Calculated k_{eff}	$\Delta V/V$ †	q ††
1	0.30	528	47.7	118.8	0.40	0.966	676	134.4	0.36	0.980	0.219	0.065
	0.49	455	59.2	98.9	0.60	0.973	560	109.8	0.54	0.988	0.188	0.081
	0.68	432	70.3	88.5	0.80	0.975	533	98.3	0.72	0.992	0.189	0.090
	0.78	433	76.2	85.1	0.89	0.976	570	97.9	0.78	0.999	0.240	0.100
	0.97	436	87.6	79.6	1.10	0.974	532	87.9	1.00	0.994	0.180	0.111
	1.32	466	110.2	73.4	1.50	0.972	576	81.6	1.35	0.995	0.191	0.120
	1.97	561	153.5	68.2	2.25	0.970	694	75.9	2.02	0.995	0.192	0.130
	0.90***	560	83.6	92.8	0.90	0.999	-	-	-	-	-	-
	sphere	560	-	102.2	-	1.0009	-	-	-	-	-	-
2	0.27	1374	54.0	180.0	0.30	0.985	1868	210.0	0.20	1.004	0.264	0.072
	0.36	1039	59.6	149.0	0.40	0.979	1206	160.5	0.37	0.992	0.139	0.094
	0.57	896	74.4	123.9	0.60	0.987	1042	133.6	0.56	1.004	0.140	0.121
	0.76	850	87.9	111.0	0.79	0.988	983	119.3	0.74	1.007	0.135	0.140
	0.87	853	95.7	106.6	0.90	0.990	917	110.5	0.87	1.000	0.070	0.143
	0.96	850	102.7	102.7	1.00	0.989	985	110.5	0.93	1.010	0.137	0.152
	1.44	919	138.0	92.1	1.50	0.986	1062	99.0	1.39	1.010	0.135	0.176
	2.16	1110	192.6	85.7	2.25	0.985	1276	91.8	2.10	1.009	0.130	0.183
	0.92***	918	99.6	108.3	0.92	1.0008	-	-	-	-	-	-
	sphere	850	-	117.5	-	1.0002	-	-	-	-	-	-
3	0.32	650	42.1	140.2	0.30	1.008	690	144.4	0.29	1.014	0.058	0.104
	0.45	473	49.6	110.3	0.45	0.998	490	112.2	0.44	1.003	0.035	0.143
	0.59	414	57.5	95.8	0.60	0.993	429	97.4	0.59	0.999	0.035	0.171
	0.78	384	67.9	84.9	0.80	0.989	398	86.4	0.79	0.996	0.035	0.200
	1.17	396	89.9	74.9	1.20	0.990	412	76.4	1.18	0.999	0.039	0.231
	1.48	423	106.6	71.1	1.50	0.992	441	72.6	1.47	1.002	0.041	0.243
	sphere	377	-	89.6	-	1.000	-	-	-	-	-	-
4	0.50	455	59.2	98.9	0.60	0.974	560	109.8	0.54	0.989	0.188	0.080
	0.68	432	70.3	88.4	0.80	0.975	533	98.3	0.72	0.993	0.189	0.095
	0.78	433	76.2	84.6	0.90	0.976	570	97.6	0.78	1.000	0.240	0.100
	0.96	435	87.6	79.6	1.10	0.975	531	87.9	1.00	0.994	0.181	0.105
	1.32	466	110.2	73.4	1.50	0.973	576	81.6	1.35	0.996	0.191	0.120
	sphere	544	-	101.3	-	1.000	-	-	-	-	-	-

*Core height (L) is the same for "First" and "Second" Calculation.

**L/D = core height/core diameter

***Cylindrical core size predicted from spherical calculation and curves on Figs. 4 and 5.

† $\Delta V/V \equiv (V_2 - V_1)/V_2$

†† $q \equiv (\Delta k/k)/(\Delta M/M) = \left(\frac{k_2 - k_1}{k_2}\right) \Big/ \left(\frac{M_2 - M_1}{M_2}\right)$

Table IV

SUMMARY OF SHAPE FACTOR ANALYSES*

Reactor No.	L/D	V (liters)**	Shape Factor	Reactor No.	L/D	V (liters)**	Shape Factor
1	0.30	946	0.591	3	0.32	586	0.643
	0.49	678	0.826		0.45	480	0.785
	0.68	590	0.948		0.59	431	0.875
	0.78	571	0.980		0.78	406	0.928
	0.97	566	0.988		1.17	414	0.911
	1.32	602	0.930		1.48	437	0.863
	1.97	732	0.765				
2	0.27	1696	0.501	4	0.50	662	0.821
	0.36	1283	0.661		0.68	581	0.936
	0.57	993	0.855		0.78	570	0.954
	0.76	923	0.920		0.96	569	0.956
	0.87	909	0.934		1.32	599	0.908
	0.96	923	0.920				
	1.44	995	0.853				
	2.16	1203	0.705				

*Data based on calculations in Table III.

**Core Volume.

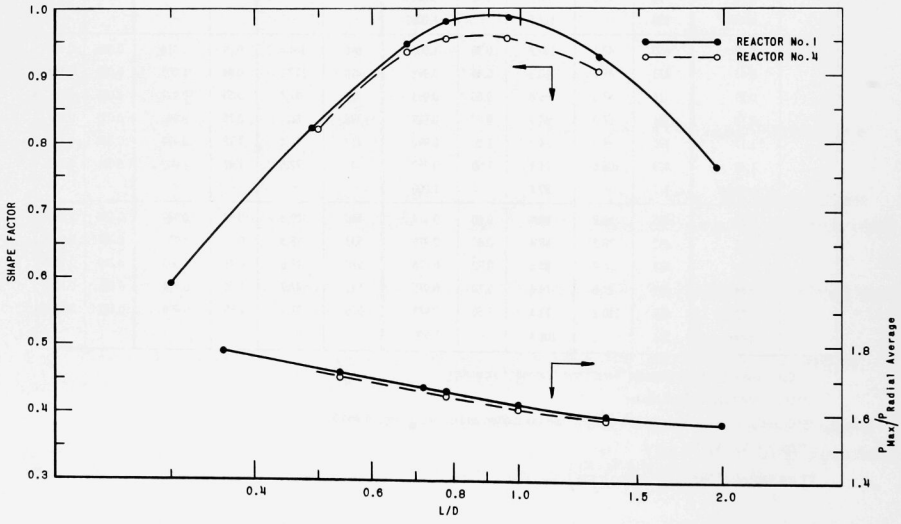

FIG. 4
SHAPE FACTORS FOR HIGH DENSITY CORES

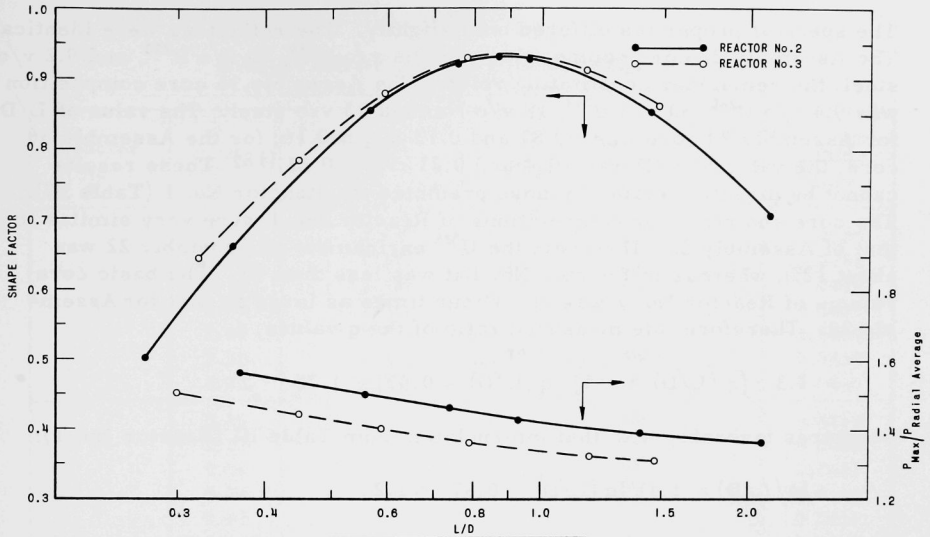

FIG. 5
SHAPE FACTORS FOR LOW DENSITY CORES

IV. PERTURBATIONS AT RADIAL CORE BOUNDARY AS A FUNCTION OF CORE GEOMETRY

The last column of Table III gives a parameter related to the predicted worth of fuel (core material) at the core boundary. The coefficient relating fractional change in critical mass with reactivity is given by the equation

$$\frac{\Delta k}{k} \approx q \frac{\Delta M}{M} \quad ,$$

where k is the effective multiplication constant and M the critical mass, and is a fairly sensitive function of L/D. It is to be noted that the relationship between reactivity $\Delta k/k$ and the fraction of fuel substituted at the core boundary, $\Delta M/M$, is, in general, nonlinear. Therefore, the calculated "q" values in Table III are peculiar to the indicated increments of substitution, $\Delta V/V$.

The calculations showed that, over a large range, $q \sim \ln (L/D)$. This result was experimentally confirmed[18] in the ZPR-III Shape Factor experiments.[1] Furthermore, the measurements of q with ZPR-III Assemblies-22 and 36[2,18] confirmed the conclusion that q is a sensitive function of L/D. The critical masses of these two assemblies differed by less than 2 kg U^{235}.

The spectral properties differed only slightly. The reflectors were identical. The Assembly 22 core composition was 9.4 v/o U^{235}, 70 v/o U^{238}, and 9.2 v/o steel, the remainder constituting voids. The Assembly 36 core composition was 9.4 v/o U^{235}, 50 v/o U^{238}, 18 v/o Na, and 13 v/o steel. The value of L/D for Assembly 22 core was ~0.87 and $0.13 \leq q \leq 0.16$; for the Assembly 36 core, the value of L/D was ~1.4 and $0.21 \leq q \leq 0.23$.[18] These results cannot be directly related to those predicted for Reactor No. 1 (Table III). The core and reflector compositions of Reactor No. 1 were very similar to that of Assembly 22. However, the U^{235} enrichment of Assembly 22 was about 12%, whereas in Reactor No. 1 it was less than 9%. The basic core volume of Reactor No. 1 was about four times as large as that for Assembly 22. Therefore, the measured ratio of the q values,

$$1.3 < [q\,(L/D) \approx 1.4]/[q\,(L/D) \approx 0.87] < 1.75 \quad ,$$

compares favorably with that interpolated from Table III (Reactor No. 1):

$$[q\,(L/D) \approx 1.4]/[q\,(L/D) \approx 0.87] \approx 1.2 \quad .$$

This comparison is only intended to show experimental verification of the predicted variation of q with L/D.

An absolute comparison of predicted with measured values of q can be obtained from ZPR-III Assembly 25. The experimental core with $L/D \approx 0.9$ gave $q \approx 0.13$, whereas interpolation of data in Table III gives $q \approx 0.11$ for Reactor No. 1. This difference of ~20% between theory and experiment is expected. The use of the three-group constants (Table II) tends to overpredict the critical mass by about 20%. The error in the calculated multiplication constant is about 2% $\Delta k/k$.

V. POWER DISTRIBUTION AS A FUNCTION OF CORE GEOMETRY

The four reactor analyses also yield information on the power distribution as a function of core geometry. In particular, the various maximum-to-average power densities may be obtained from the calculations. Such ratios are given in Table V. For the most part, it is seen that they are only slowly varying functions of changes in L/D. The more significant and interesting of these are the ratios of maximum power density to average radial power density, which are also shown on Figs. 4 and 5. It should be noted that the largest value of this ratio is predicted for small values of L/D. Also, the variation of this quantity as a function of L/D is much more pronounced than for the other power parameters in Table V.

Table V

VARIATION OF POWER PRODUCTION WITH CYLINDRICAL CORE GEOMETRY (L/D)

Reactor No.	L/D	$\left(\frac{P_{max}}{P_{ave}}\right)_{core}$ *	$\left(\frac{P_{max}}{P_{radial\ ave}}\right)_{core}$ **	$\frac{P_{refl}}{P_{core}}$ †
1	0.36	2.21	1.78	0.0529
	0.54	2.18	1.71	0.0448
	0.72	2.18	1.67	0.0446
	0.78	2.19	1.66	0.0425
	1.00	2.17	1.62	0.0439
	1.35	2.18	1.59	0.0439
	2.02	2.23	1.57	0.0440
2	0.20	2.09	1.75	0.0519
	0.37	2.00	1.66	0.0500
	0.56	1.97	1.60	0.0461
	0.74	1.96	1.56	0.0450
	0.87	1.95	1.54	0.0440
	0.93	1.96	1.52	0.0444
	1.39	1.98	1.49	0.0444
	2.10	2.02	1.46	0.0448
3	0.30	1.72	1.51	0.147
	0.45	1.65	1.44	0.149
	0.59	1.62	1.40	0.146
	0.79	1.61	1.36	0.147
	1.18	1.62	1.34	0.146
	1.47	1.64	1.31	0.144
4	0.54	2.17	1.70	0.0276
	0.72	2.16	1.67	0.0267
	0.78	2.17	1.64	0.0256
	1.00	2.16	1.61	0.0263
	1.35	2.19	1.58	0.0268

*P_{max} = Maximum Power Density (at center of core)

$$P_{ave} = \int_{core} P(r,z)\, dV \Big/ \int_{core} dV$$

$$**P_{radial\ ave} = \int_{core} P(r,o)\, rdr \Big/ \int_{core} rdr$$

$$^{\dagger}P_{core} = \int_{core} P(r,z)\, dV$$

$$P_{refl} = \int_{reflector} P(r,z)\, dV$$

The power data for Reactor No. 1 were compared with axial fission distributions* measured with ZPR-III Assembly 25. These results are shown on Figs. 6 and 7. The experimental results were normalized to the predicted data at the center of the core. The comparison between theory and experiment is good enough to support the predictions in Table V.

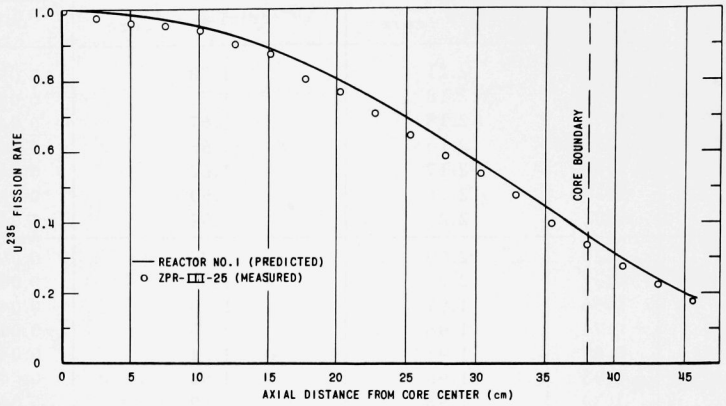

FIG. 6
AXIAL U^{235} FISSION DISTRIBUTION
ON CORE CENTERLINE

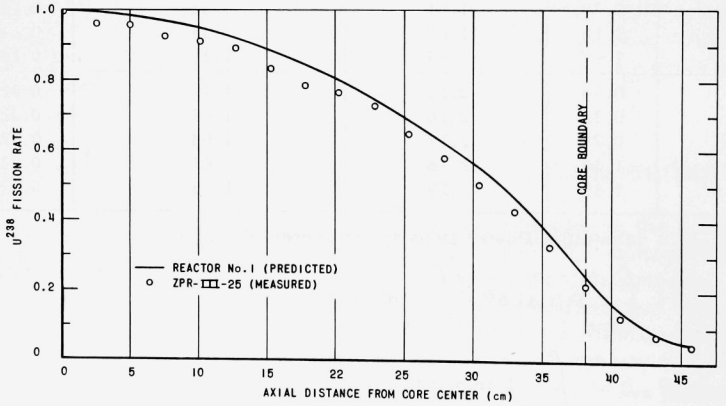

FIG. 7
AXIAL U^{238} FISSION DISTRIBUTION
ON CORE CENTERLINE

* These distributions were measured along the axis of symmetry.

VI. INTERPRETATION OF THE ANALYTICAL RESULTS

The net neutron leakage from the core is an important contributor to the Shape Factor determination. It is reasonable, therefore, to expect that the Shape Factor be strongly dependent upon the ratio of the spherical core surface area to the cylindrical core surface area.* The results from Table IV were reinterpreted on such a basis and are shown on Fig. 8. The Shape Factor is given as a function of S_s/S_c, where S_s and S_c are the appropriate spherical and cylindrical core surface areas, respectively. Figure 9 gives similar results for the experimentally investigated moderately sized cores.(1)

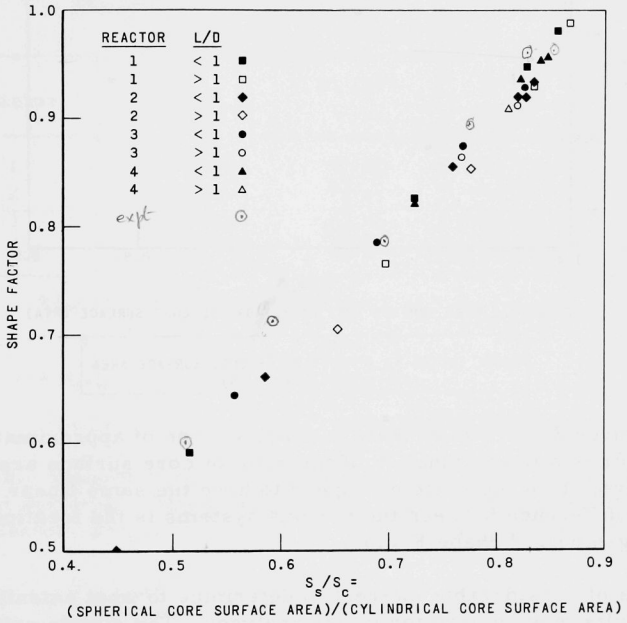

FIG. 8
SHAPE FACTOR AS A FUNCTION OF CORE SURFACE AREA
(ANALYTICAL RESULTS)

* Table V shows that the ratio of maximum to average power density as a function of core geometry does not vary by more than 7.5%.

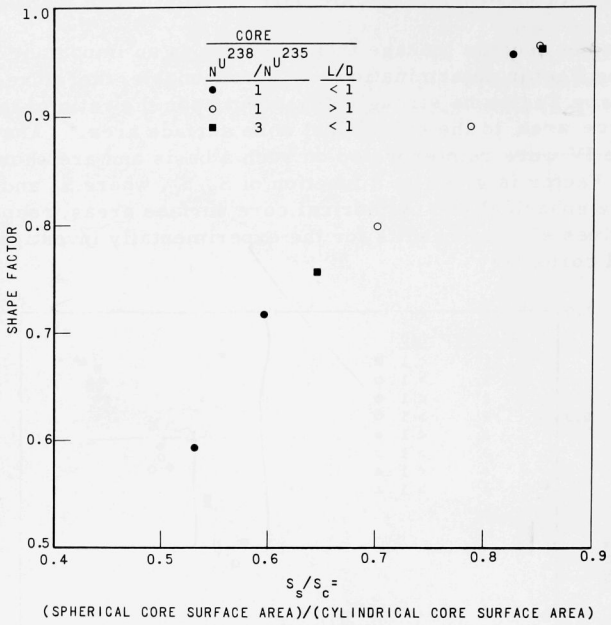

FIG. 9
SHAPE FACTOR AS A FUNCTION OF CORE SURFACE AREA
(EXPERIMENTAL RESULTS)

Figures 8 and 9 show that, to a high degree of approximation, the Shape Factor is a linear function of the ratio of core surface areas.* Furthermore, all of the systems appear to have the same linear dependence. The major difference between the various systems is the location of the "optimum geometry" Shape Factor.

It is of considerable interest to determine to what extent rather simple results may be used for future analyses. The simple criticality equation

$$\kappa^2 = \left(\frac{\pi}{S + s}\right)^2 = \left(\frac{2.405}{R + \delta}\right)^2 + \left(\frac{\pi}{L + 2\Delta}\right)^2 \quad , \tag{5}$$

where S, R, and L are the calculated spherical radius, cylindrical radius and core height, respectively,** and s, δ and Δ are the spherical, radial cylindrical and axial cylindrical "reflector savings," respectively, was

* Comparing core surface to volume ratios of cylindrical with spherical systems does not yield such a simple dependence.

** Spherical results from Table III; cylindrical results from Table IV.

applied to the results of the detailed analytical results. The criticality condition requires that the material buckling κ^2 be equated to the geometric buckling. The material buckling is obtained from a diffusion theory fundamental mode calculation. The "reflector saving" as used here is the actual reflector saving plus extrapolation distance.

Table VI summarizes the reflector saving determinations for the spherical systems along with the calculated material bucklings.

Table VI

MATERIAL BUCKLINGS AND SPHERICAL CORE REFLECTOR SAVINGS

Reactor	κ^{2*} (cm^{-2})	S + s** (cm)	S*** (cm)	s† (cm)
1	0.002515	62.64	51.13	11.5
2	0.001613	78.22	58.77	19.5
3	0.002013	70.02	44.81	25.2
4	0.002515	62.64	50.64	12.0

* Calculated material buckling

** $S + s = \pi/\kappa$

*** From Table III

†Reflector Saving plus Extrapolation Distance

Table VII summarizes the reflector saving determinations for the cylindrical systems. These were obtained by assuming that the axial and radial reflector savings are equal. Equation (5) was reordered as follows:

$$\left[(R + \delta)^2 - \gamma^2\right]\left[(L + 2\Delta)^2 - \epsilon^2\right] = \gamma^2 \epsilon^2 \quad , \tag{6}$$

where

$$\gamma \equiv (2.405)/\kappa$$

and

$$\epsilon \equiv \pi/\kappa \quad .$$

By assuming $\delta = \Delta$, the resulting fourth-order equation was solved for the single real and positive root. Table VII summarizes these calculations.

Table VII

REFLECTOR SAVING† DETERMINATIONS FOR CYLINDRICAL CORES

(Axial and radial reflector savings are assumed equal)

Reactor	L/D	D (cm)	s†† (cm)	$\Delta = \delta^*$ (cm)	$\Delta = \delta^{**}$ (cm)	Δ^{***}	Approx. Error**** (%)
1	0.30	158.94	11.5	12.8	13.9	14.7	+3.0
	0.49	120.78		12.2	13.4		
	0.78	97.68		12.3	13.7		
	0.97	90.56		12.4	13.7		
	1.32	82.96		12.7	13.8		
2	0.27	199.98	19.5	18.4	20.4	21.7	-2.2
	0.36	165.56		18.7	21.4		
	0.76	115.64		18.8	22.1		
	0.87	109.98		18.9	22.1		
	0.96	106.98		18.7	21.7		
	1.44	95.82		19.0	21.3		
	2.16	89.18		19.1	20.7		
3	0.32	132.60	25.2	22.6	30.3	27.1	-4.8
	0.45	110.74		23.1	32.9		
	0.59	97.62		23.4	34.5		
	0.78	87.18		23.8	35.0		
	1.17	76.66		23.9	32.9		
	1.48	72.68		25.4	30.8		
4	0.50	119.02	12.0	12.3	13.6	15.6	+1.0
	0.68	102.84		12.5	13.9		
	0.78	97.62		12.4	13.7		
	0.96	91.04		12.3	13.6		
	1.32	83.28		12.5	13.6		

*Exact solution of Equation (7).

**Neglect cubic and quartic terms in Equation (7).

***Evaluation of:

$$\delta \approx \Delta \approx \frac{1}{\kappa} \tan^{-1}\left\{ \frac{\sum_{tr}^{ref}}{\sum_{tr}^{core}} \kappa L_{ref} \right\}$$

****Error incurred by using spherical reflector saving in cylindrical calculation with optimum L/D.

$$\text{Error} = E \approx 3 \frac{\Delta - s}{D} .$$

†Reflector saving includes extrapolation length.

††Spherical reflector saving from Table VI.

Table VII also gives the results of neglecting the coefficients of the cubic and quartic terms for Δ in Equation (6). This approximation becomes better as the ratio of core dimension to reflector saving increases. This is simply because expansion of Equation (6) gives the following:

$$\Delta^4 + 2\Delta^3 D\left[1 + \frac{L}{D}\right] + \Delta^2 D^2\left[1 + 4\frac{L}{D} + \left(\frac{L}{D}\right)^2 - \frac{1}{D^2}(q + Q)\right]$$

$$+ 2\Delta D^3\left[\frac{L}{D} + \left(\frac{L}{D}\right)^2 - \frac{1}{D^2}\left(q\frac{L}{D} - Q\right)\right] + D^4\left[\left(\frac{L}{D}\right)^2 - \frac{q\left(\frac{L}{D}\right)^2 + Q}{D^2}\right] = 0 \qquad (7)$$

where

$\delta = \Delta$

$q = 4\left(\frac{2.405}{\kappa}\right)^2$

$Q = (\pi/\kappa)^2$

$D = 2R$ = core diameter;

L = core height.

It may be seen on Table VII that the easily obtained spherical reflector saving from Table VI may not be used for high-precision cylindrical calculations. The spherical reflector saving is less than the exact cylindrical value for the high-density cores (Reactors 1 and 4) and is greater than the exact cylindrical value for the low-density cores (Reactors 2 and 3).

The reflector savings for an infinite slab reactor with reflector (Formula 3.212.2 of Ref. 19) is given by

$$\delta = \frac{1}{\kappa}\tan^{-1}\left\{\frac{\sum_{tr}^{ref}}{\sum_{tr}^{core}}\kappa L_{ref}\right\}, \qquad (8)$$

where

$\sum_{tr}^{core}$ and $\sum_{tr}^{ref}$ are spectrum-averaged transport cross sections for

Table VIII

REFLECTOR SAVING DETERMINATIONS BY CORRELATING ONE- AND TWO-DIMENSIONAL ANALYSES

Reactor No.	L/D	R* (cm)	L** (cm)	b_r^2 † ($\times 10^{+3}$) (cm^{-2})	b_z^2 †† ($\times 10^{+3}$) (cm^{-2})	$\kappa^2 = b_r^2 + b_z^2$ ($\times 10^{+3}$) (cm^{-2})	R + δ† (cm)	L + 2Δ†† (cm)	δ*** (cm)	Δ††† (cm)
1	.30	79.47	47.68	0.5488	1.7969	2.3457	102.66	74.07	23.2	13.2
	.49	60.39	59.18	1.0472	1.3856	2.4328	74.32	84.36	13.9	12.6
	.68	51.70	70.31	1.3698	1.0609	2.4307	64.98	96.40	13.3	13.0
	.78	48.85	76.20	1.4996	0.9356	2.4352	62.10	102.65	13.3	13.2
	.97	45.28	87.84	1.6971	0.7229	2.4200	58.38	116.78	13.1	14.6
	1.32	41.72	110.14	1.9399	0.4807	2.4206	54.61	143.22	12.9	16.5
	1.97	38.96	153.50	2.1761	0.2615	2.4376	51.56	194.18	12.6	20.3
	F.M.[a]					2.515			11.5	
2	.27	99.99	53.99	0.3995	1.2018	1.6013	120.33	90.57	20.3	18.3
	.36	82.79	59.61	0.5403	1.0514	1.5917	103.47	96.84	20.7	18.6
	.57	65.22	74.35	0.8095	0.7908	1.6002	84.53	111.66	19.3	18.7
	.76	57.82	87.89	0.9756	0.6317	1.6073	76.99	124.94	19.2	18.5
	.87	55.00	95.70	1.0447	0.5605	1.6052	74.41	132.63	19.4	18.5
	.96	53.49	102.70	1.1094	0.5136	1.6230	72.21	138.56	18.7	17.9
	1.44	47.92	138.01	1.2860	0.3204	1.6065	67.06	175.41	19.1	18.7
	2.16	44.59	192.63	1.4252	0.1850	1.6102	63.70	230.89	19.1	19.1
	F.M.[a]					1.613			19.5	
3	.32	66.30	42.43	0.7318	1.3432	2.0750	88.91	85.68	22.6	21.6
	.45	55.37	49.83	0.9409	1.1314	2.0723	78.41	93.35	23.0	21.8
	.59	48.81	57.60	1.1094	0.9725	2.0819	72.21	100.69	23.4	21.5
	.78	43.59	68.00	1.2831	0.7935	2.0765	67.14	111.47	23.6	21.7
	1.17	38.33	89.69	1.5000	0.5616	2.0616	62.10	132.50	23.8	21.4
	1.48	36.10	106.85	1.6126	0.4406	2.0532	59.89	149.60	23.8	21.4
	F.M.[a]					2.013			25.2	
4	.50	59.51	59.51	1.0718	1.3521	2.4239	73.46	85.39	14.0	12.9
	.68	51.42	69.93	1.3663	1.0482	2.4145	65.06	96.99	13.6	13.5
	.78	48.82	76.16	1.4996	0.9212	2.4209	62.10	103.45	13.3	13.6
	.96	45.52	87.40	1.7011	0.7462	2.4473	58.31	114.95	12.8	13.7
	1.32	41.64	109.93	1.9459	0.4823	2.4283	54.52	142.97	12.9	16.5
	F.M.[a]					2.515			12.0	

*Used in radially reflected axially bare cylindrical calculation.

**Used in axially reflected radially bare slab calculation.

***Radial reflector saving plus extrapolation length.

†Obtained from axially reflected radially bare slab calculation.

††Obtained from radially reflected axially bare cylindrical calculation.

†††Axial reflector saving plus extrapolation length.

[a]F.M. = Fundamental Mode Analysis (From Table VI)

core and reflector, respectively, and L_{ref} is the spectrum-averaged reflector diffusion length.

The results of evaluating Equation (8) for the four reactor systems are also shown in Table VII. The core spectrum from the fundamental mode calculations was used to average both core and reflector constants. The core leakage spectrum into the blanket is more like the core spectrum than the asymptotic blanket spectrum. Therefore, a spectrum harder than the asymptotic blanket spectrum will be significant toward the reflector saving determination. It may be seen from Table VII that the evaluation of Equation (8) consistently overpredicts the reflector saving.

It is of interest to see what error is introduced through the use of the spherical reflector saving in a cylindrical calculation. This error is predicted for near optimum geometry systems. The error is approximately given by

$$\text{Error in core size}^{*} = E \approx 3 \frac{\Delta\text{-}s}{D} \quad .$$

The last column in Table VII shows the result of these calculations.

One-dimensional calculations were used to determine the variation of both axial and radial reflector saving with core geometry. Core radii and diameters were specified from the calculated two-dimensional critical systems cited in Tables IV and VII. Then a series of radially reflected cylindrical calculations were brought critical by varying the axial buckling. Similarly, a series of axially reflected slab calculations were brought critical by varying the radial buckling. The bare core radii and heights extracted from the transverse bucklings then yielded the reflector savings (plus extrapolation distance). This was accomplished by subtracting the reflected core radii and heights, respectively, obtained from the two-dimensional calculations. Table VIII summarizes the results of this approach.

It is significant to note that the sum $b_r^2 + b_z^2 \equiv \kappa^2$, although relatively constant as a function of L/D, does not agree with the results of the fundamental mode analysis (Table VI)** Values of κ^2 from the latter are 2.515, 1.613, 2.013, and 2.515×10^{-3} for Reactors 1, 2, 3, and 4, respectively. The difference between the values of κ^2 in Table VIII and those from Table VI are indicative of the limitations of purely one-dimensional calculations coupled with fundamental mode analyses.

---

* $L/D \approx 1$.

** These are also shown on Table VIII.

The extracted reflector savings δ and Δ in Table VIII show a significant variation as a function of L/D. In general, axial and radial reflector savings are not equal. Occasional small deviations from smooth variation as a function of L/D occur. These must be attributed to the difference in convergence criteria between the various analyses used in the calculation. In general, the one-dimensional calculations converged better than the two-dimensional analyses. The one-dimensional method shows gross errors only for systems near the extremities of the analyses; those having either very high or very low ratios of core height to diameter. This is caused by the spectral influence of the reflector.

VII. CONCLUSIONS

This study extends existing experimental Shape Factor data by analysis of four conceptual systems. The major practical implications of the analysis are:

1. Shape Factors are more dependent upon core than reflector composition.

2. The Shape Factors for optimum geometry (L/D ~0.9) increase with core density.

3. The reactivity worth of fuel at the core boundary tends to increase with L/D.

4. The ratio of maximum power density to average radial power density tends to be inversely proportional to ln(L/D).

If the increased fuel inventory of nonoptimum core geometry can be tolerated, there may be some definite improvement in several aspects of reactor performance. For example, reactor control may be affected by movement of fuel (or other materials) at or near the core boundary. The q values determined suggest that the reactivity held by a given amount of fuel increases almost linearly with ln(L/D). Therefore, a given amount of reactivity (for burnup or shutdown) may be more easily provided in nonoptimum core geometry with $L/D > 1$.

The predicted positive sodium void coefficient[15] may be effectively reduced or brought negative in nonoptimum geometry. This study shows that, under proper conditions, other advantageous control and engineering features may accompany the nonoptimum geometry core design.

The study also shows that some care must be taken in assigning Shape Factors for precision comparison between spherical calculations and cylindrical experiment.

It is recognized that two-dimensional analyses are required to resolve specific problems. The determination of the optimum geometry Shape Factor for a specific system is an example requiring two-dimensional analysis. However, the more approximate one-dimensional method should not be underestimated. In general, these do show the significant trends and only small errors are incurred by their use.

The approximately linear dependence between the Shape Factor and the ratio of spherical to cylindrical core surface area is demonstrated. This approximation may be confidently used to determine trends.

VIII. ACKNOWLEDGEMENTS

The authors are grateful to Dr. B. I. Spinrad for stimulating parts of this study. Helpful discussions with Dr. D. Meneghetti served to reslove some computing difficulties. Mr. J. White performed some of the detailed calculations in this report.

IX. REFERENCES

1. J. K. Long et al., Fast Neutron Power Reactor Studies with ZPR-III, Proceedings of the Second United Nations International Conference on the Peaceful Uses of Atomic Energy, Geneva, Switzerland, 12, 119 (1958).

2. J. K. Long et al., Experimental Results on Large Dilute Fast Critical Systems with Metallic and Ceramic Fuels, Paper Presented at IAEA Sponsored Seminar on the Physics of Fast and Intermediate Reactors, Vienna, 1961, Paper SM-18/48.

3. W. B. Loewenstein and D. Okrent, The Physics of Fast Power Reactors, A Status Report, Proceedings of the Second United Nations International Conference on the Peaceful Uses of Atomic Energy, Geneva, Switzerland, 12, 16 (1958).

4. S. Yiftah, D. Okrent and P. A. Moldauer, Fast Reactor Cross Sections, Pergamon Press (1960).

5. D. Meneghetti, Recent Advances and Problems in Theoretical Analyses of ZPR-III Fast Critical Assemblies, Paper Presented at IAEA Sponsored Seminar on the Physics of Fast and Intermediate Reactors, Vienna, 1961, Paper No. SM-18/37.

6. G. E. Hansen, Properties of Elementary Fast Neutron Critical Assemblies, Proceedings of the Second United Nations International Conference on the Peaceful Uses of Atomic Energy, Geneva, Switzerland, 12, 84 (1958).

7. G. E. Hansen, Status of Computational and Experimental Correlations for Los Alamos Fast Neutron Critical Assemblies, Paper Presented at IAEA Sponsored Seminar on the Physics of Fast and Intermediate Reactors, Vienna, 1961, Paper No. SM-18/53.

8. Reactor Physics Constants, ANL-5800 (1958).

9. H. H. Hummel and A. L. Rago, An Accurate Treatment of Resonance Scattering in Light Elements in Fast Reactors, Paper Presented at IAEA Sponsored Seminar on the Physics of Fast and Intermediate Reactors, Vienna, 1961, Paper No. SM-18/45.

10. F. Kloverstrom, Spherical and Cylindrical Plutonium Critical Masses, UCRL-4957 (Sept 1957).

11. V. Josephson, R. W. Paine, Jr., and L. L. Woodward, Oralloy Shape Factor Measurements, LA-1155 (1950).

12. E. C. Malary, Oralloy Cylindrical Shape Factor and Critical Mass Measurements in Graphite, Paraffin, and Water Tampers, LA-1305 (1951).

13. L. J. Koch et al., Construction Design of the EBR-II: An Integrated Unmoderated Nuclear Power Plant, Proceedings of the Second United Nations International Conference on the Peaceful Uses of Atomic Energy, Geneva, Switzerland, 9, 323 (1958).

14. W. B. Loewenstein, The Physics Design of the EBR-II, Paper Presented at IAEA Sponsored Seminar on Fast and Intermediate Reactors, Vienna, 1961, Paper No. SM-18/39.

15. D. Okrent, Performance of Large Fast Power Reactors Including Effects of Higher Isotopes, Recycling and Fission Products, Paper Presented at IAEA Sponsored Seminar on the Physics of Fast and Intermediate Reactors, Vienna, 1961, Paper No.SM-18/41.

16. G. G. Bilodeau et al., PDQ - An IBM 704 Code to Solve the Two-dimensional Few Group Neutron Diffusion Equations, WAPD-TM-70 (1957).

17. M. K. Butler and J. M. Cook, Univac Program for the Solution of One-dimensional Multigroup Reactor Equations, ANL-5437 (1954) [RE-122 is the same program executed on the IBM-704].

18. Private Communication, J. M. Gasidlo, ANL-ZPR-III.

19. S. Glasstone, Principles of Nuclear Reactor Engineering, D. Van Nostrand Co., New York (1955).